Physica A 591 (2022) 126799

Contents lists available at ScienceDirect

Physica A

journal homepage: www.elsevier.com/locate/physa

Spreading processes in "post-epidemic" environments. II. Safety patterns on scale-free networks

V. Blavatska [a,b,*], Yu. Holovatch [a,b,c]

[a] Institute for Condensed Matter Physics of National Acad. Sci. of Ukraine, Lviv, Ukraine
[b] L^4 Collaboration & Doctoral College for the Statistical Physics of Complex Systems, Leipzig-Lorraine-Lviv-Coventry, Europe
[c] Centre for Fluid and Complex Systems, Coventry University, Coventry, CV1 5FB, United Kingdom

ARTICLE INFO

Article history:
Received 7 October 2021
Received in revised form 11 December 2021
Available online 22 December 2021

MSC:
92D30
37B15
82B43

Keywords:
Spreading
Complex networks
Epidemiology
Cellular automaton

ABSTRACT

This paper continues our previous study on spreading processes in inhomogeneous populations consisting of susceptible and immune individuals (Blavatska and Holovatch, 2021). A special role in such populations is played by "safety patterns" of susceptible nodes surrounded by the immune ones. Here, we analyze spreading on scale-free networks, where the distribution of node connectivity k obeys a power-law decay $\sim k^{-\lambda}$. We assume, that only a fraction p of individual nodes can be affected by spreading process, while remaining $1-p$ are immune. We apply the synchronous cellular automaton algorithm and study the stationary states and spatial patterning in SI, SIS and SIR models in a range $2 < \lambda < 3$. Two immunization scenarios, the random immunization and an intentional one, that targets the highest degrees nodes are considered. A distribution of safety patterns is obtained for the case of both scenarios. Estimates for the threshold values of the effective spreading rate β_c as a function of active agents fraction p and parameter λ are obtained and efficiency of both vaccination techniques is analyzed quantitatively. The impact of the underlying network heterogeneous structure is manifest e.g. in decreasing the β_c values within the random scenario as compared to corresponding values in the case of regular lattices. This result quantitatively confirms the compliance of scale-free networks for disease spreading. On contrary, the vaccination within the targeted scenario makes the complex networks much more resistant to epidemic spreading as compared with regular lattice structures.

1. Introduction

The concept of complex networks is widely used to describe both the nature and society; many systems can be treated as graphs with nodes representing individuals or agents and links displaying any kind of mutual interactions between them. The question of great interest it thus the impact of complex network topology on the dynamics of spreading phenomena on such structures [1], ranging from computer virus [2,3] to rumor spread [4] and to infectious diseases [5]. Of particular importance in this respect are the so-called scale-free (SF) networks [6], where the node degree distribution $P(k)$ is governed by a power-law decaying:

$$P(k) \sim k^{-\lambda}, \qquad k \gg 1\,. \tag{1}$$

* Corresponding author at: Institute for Condensed Matter Physics of National Acad. Sci. of Ukraine, Lviv, Ukraine.
E-mail address: blavatskav@gmail.com (V. Blavatska).

https://doi.org/10.1016/j.physa.2021.126799
0378-4371/

It is established, that a number of important real networks such as WWW [7–9], collaboration and co-authorship [6,10], food web and trophic interactions in ecosystems [11] etc. are characterized by distribution (1) with exponent λ in a range $2 < \lambda < 3$.

The spreading processes on SF networks have been thoroughly analyzed, in particular, within the frames of archetype scenarios of epidemics invasion (based on the so-called compartment models [12,13] considered in more details in Section 3.1). Such networks are found to be highly compliant to spreading processes [14–17]. It is caused by diverging connectivity fluctuations of SF networks with $\lambda < 3$ (in the asymptotic limit of infinitely large networks, the second moment $\langle k^2 \rangle$ of the degree distribution (1) diverges) and by a statistically significant probability for some nodes to have a very high degree compared to the mean one. Note however that for smaller size networks $\langle k^2 \rangle$ has a large but finite value, defining an effective nonzero threshold for epidemic outbreak in such systems due to the finite size effects, as it is usual in non-equilibrium phase transitions [18]. An impressive research effort has been devoted to deeper understanding of the spreading dynamics on complex SF networks, including degree-based mean-field theories [14,15,19–22], exact methods [23,24] and numerical simulations [20,21,25,26], see Ref. [17] for a recent review.

Since the infection with 100% efficiency is not realistic even for highly virulent diseases, it is reasonable to use a model in which only some fraction p of nodes are considered susceptible to the disease transmission. One can observe such a case e.g. in population, where $1 - p$ individuals has become immune, whether through vaccination or being infected and cured previously. Immunization strategies protect the population from the global propagation of a disease and can also lead to an increase of the epidemic threshold (this effect is called herd immunity) [27]. In our previous work [28], such a situation was considered by studying the stationary states and spatial patterning on a square lattice with the fraction p of susceptible to disease transmission (active) sites. An emergence of "safety patterns" of susceptible agents surrounded by immune individuals in such a system was described quantitatively. This concept plays an important role in the course of epidemic processes and determines the fraction of infected agents in a stationary state. Estimates for the threshold values of epidemic outbreak as a function of active agents fraction p on a square lattice were obtained by us as well.

The present work serves as a continuation of the study, initiated in [28] generalizing it for the case of SF networks with node degree distribution given by (1) with exponent λ in a range $2 < \lambda < 3$. The fraction p of nodes are considered as susceptible for disease spreading, whereas the rest $1 - p$ are treated as immune. Various immunization scenarios can be performed in such networks due to their heterogeneity. The simplest (and not effective one) is the random immunization, in which a number $(1 - p)N$ of nodes is randomly chosen and made immune. For the infinite networks it was proven [29] that almost the whole network must be immunized to suppress the disease. More effective level of protection in SF networks is achieved by means of optimized immunization strategies, targeting the highest degree nodes [29–31], which are potentially the strongest spreaders. Other effective targeted immunization strategies are based e.g. on the betweenness centrality, which combines the ideas of taking into account the highest degree nodes and the most probable paths for infection transmission [32]. The immunization protocols can be improved also by allowing for each node to have information about the degree of its nearest neighbors, and thus immunizing the neighboring nodes with the largest degree [33].

The layout of the paper is as follows. In the next Section 2, we introduce the model for constructing the SF networks with desired power-law distribution (1) and analyze the general impact of vaccination (removing some amount of the active nodes) on network connectivity. In Section 3, we briefly overview possible spreading scenarios and describe the cellular automaton method, which is applied to implement them. Our main results for the quantitative description of disease spreading within two different vaccination scenarios are given in Section 4. We end up with giving Conclusions in Section 5.

2. The model

Aiming to study the infection spreading process on SF networks with a power-law degree distribution in the form (1), we make use of the so-called configuration model to construct the network and then apply two different scenarios to make some amount of nodes considered as vaccinated.

2.1. Constructing a network

Within the frames of the configuration model [34,35], we start with a set of $N = 6000$ disconnected nodes. A degree k_i ($i = 1, \ldots, N$) is assigned to each of the nodes ($\sum_i k_i$ should be an even number, since each link should connect the two nodes). The degree is given by a random number selected from probability distribution $P(k)$ with condition $k_{\min} \leq k_i \leq k_{\max}$ with desired minimal and maximal degrees, correspondingly. We take $k_{\min} = 2$ to provide connectivity of network (the existence of so-called giant connected component) [36,37].

The maximum degree cutoff $k_{\max} \sim N^{1/2}$ is introduced [38] in order to decrease the degree correlations (disassortativity) in configuration model. The actual network is constructed by randomly connecting the nodes according to the prescribed numbers of their outgoing links k_i with control of avoidance of multiple connections and self-connections. The resulting network thus contains $\sum_i k_i/2$ links.

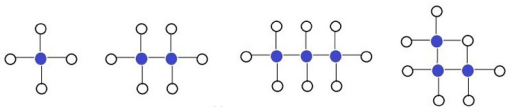

Fig. 1. Possible configurations of clusters of susceptible nodes (dark discs, blue online) up to the size $s = 3$ on a square lattice.

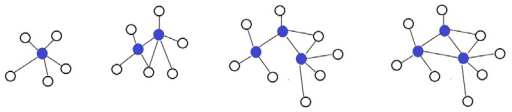

Fig. 2. Possible configurations of clusters of susceptible nodes (dark discs, blue online) up to the size $s = 3$ on a network.

2.2. Network gets vaccinated

As the next step, we assume that some fraction of nodes is immune (these nodes together with their outgoing links are removed from the lattice). In this respect, we recall the problem of the so-called node percolation on a network. The concept of the threshold probability $p_{\rm perc}$ naturally arises in such systems, such that at the concentration of remaining nodes $p < p_{\rm perc}$ the network is composed of a set of isolated disconnected clusters whereas at $p > p_{\rm perc}$ a giant cluster spans the entire network [35,36]. The percolation thresholds $p_{\rm perc}(\lambda)$ can be estimated on the basis of the general Molloy–Reed criterion for the existence of a spanning cluster [37]:

$$\frac{\langle k^2\rangle(p_{\rm perc})}{\langle k\rangle(p_{\rm perc})} = 2, \tag{2}$$

where $\langle k\rangle(p_{\rm perc})$, $\langle k^2\rangle(p_{\rm perc})$ are the mean and mean square node degree calculated at the percolation threshold.

While at $\lambda > 3$ the percolation threshold takes finite values, in the case of infinitely large networks with $\lambda \leq 3$ a spanning cluster exists at any arbitrarily small value $p > p_{\rm perc} \approx 0$. In finite systems, however, a percolation transition is observed at $\lambda \leq 3$ too, although the transition threshold $p_{\rm perc}$ is very small.

In what follows, we consider two different immunization scenarios that target either the random chosen nodes or the most "important" nodes, as explained in more details below. Let us note also that in what follows the averaging of all observables of interest is performed for each fixed p value over an ensemble of 1000 replicas of network realizations.

2.2.1. Random scenario

In the simplest scenario, we chose at random a fraction of $1 - p$ nodes and consider them as vaccinated. As a result, the network contains a number of subgraphs of s linked susceptible nodes, considered as clusters of size s. To extract clusters of different sizes numerically, we apply an algorithm developed by Hoshen and Kopelman [39]. This algorithm is successfully applied in studies of percolation phenomenon in disordered environments [40–44].

For cluster containing s nodes, let us introduce the number of such clusters per one node $n_s(p)$ [44] (the probability $P_s(p)$ to find a cluster containing s susceptible nodes is thus $P_s(p) = sn_s(p)$). Let us start with considering the case of simple square lattice with fraction p of susceptible sites (see Fig. 1). For a single susceptible site surrounded by the immune ones, as shown on the leftmost panel of Fig. 1, $n_1(p)$ is given as a probability p to find a susceptible site times probabilities of the four neighboring sites to be immune $(1 - p)^4$, so that

$$n_1(p) = p(1 - p)^4. \tag{3}$$

For the cluster of two sites, the second panel of Fig. 1, $n_2(p)$ can be calculated as a probability of two neighboring sites to be active p^2 and their six neighbors to be immune $(1 - p)^6$ taking into account that there are two such configurations (the cluster can be oriented horizontally or vertically), so that

$$n_2(p) = 2p^2(1 - p)^6. \tag{4}$$

For the cluster of three sites, the third and the fourth panels of Fig. 1, there are two possible configurations, and number of such configurations is correspondingly 2 and 4, resulting in

$$n_3(p) = p^3(2(1 - p)^8 + 4(1 - p)^7). \tag{5}$$

Applying such considerations, exact values for $n_s(p)$ with s up to 17 were obtained in Ref. [45] for a simple square lattice. For the case of complex network, the number of nearest neighbors for each node is not fixed. Following the same reasoning as those given above in the simple square lattice case, one can estimate the number of single-node ($s = 1$) clusters on a network (leftmost panel of Fig. 2),

$$n_1(p) = p(1 - p)^{\langle k\rangle} \tag{6}$$

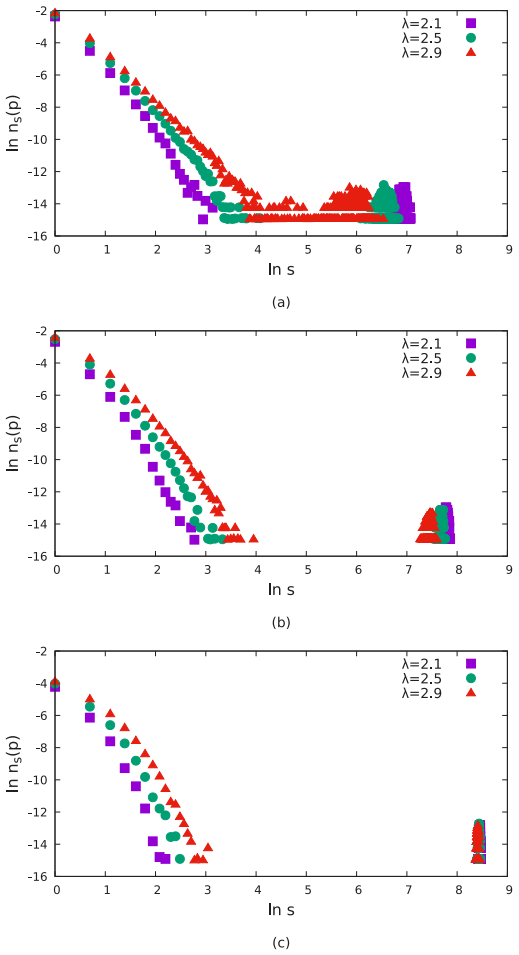

Fig. 3. Number of clusters per network node $n_s(p)$, averaged over an ensemble of network configurations, as a function of cluster size s for a SF network of size $N = 6000$ at various λ and concentrations of susceptible nodes $p = 0.3$ (a), $p = 0.5$ (b), $p = 0.8$ (c) in a double logarithmic scale. The random scenario is applied. Probability and a size of the largest component increases both with increasing of p and decreasing of λ.

with the mean node degree $\langle k\rangle$ obtained from the corresponding node distribution, while for $s = 2$ (the second panel of Fig. 2) it can be approximately estimated as

$$n_2(p) = p^2(1-p)^{2\langle k\rangle - 2}. \tag{7}$$

The exact values for $n_s(p)$ with larger s are tricky to calculate due to complicated mutual interlinking within the network.

Our simulation results for the cluster size distribution as averaged over an ensemble of constructed networks are shown in Fig. 3. Note that the percolation thresholds for given values of λ are estimated based on Eq. (2) making use of averaged values for $\langle k\rangle(p)$ and $\langle k^2\rangle(p)$ found in our simulations: $p_{\rm perc}(\lambda = 2.1) = 0.06$, $p_{\rm perc}(\lambda = 2.5) = 0.1$, $p_{\rm perc}(\lambda = 2.9) = 0.16$ (since these are values obtained for a finite system, they are not to be compared with analytical results obtained for infinite networks). Both the concentration p of susceptible nodes and the scaling law parameter λ cause essential effects on these distributions. At values of p depicted in Fig. 3 the considered networks are above the percolation threshold, and the giant connected cluster is present in the system. At small value of $p = 0.3$, a large amount of clusters of relatively small size can be still found in a system. As the value of p increases, the probability to find small clusters is decreasing, whereas the fraction of nodes in spanning clusters increases. At $p = 0.8$, the probability for a susceptible node to belong to a percolation cluster is very high. The fluctuations in sizes of large clusters emerging in a system in vicinity of percolation threshold are caused by finite system size. On the other hand, the smaller is parameter λ, the larger is the probability for a node with a very high degree (hub) to be found in the network. The presence of such nodes increases the connectivity of network in the sense, that a larger amount of nodes belong to the spanning cluster. Indeed, as we can see in Fig. 3, at each fixed p the probability for a node to belong to the largest cluster increases with decreasing λ.

2.2.2. Targeted scenario

In the second, targeted scenario (also called an intentional one, related to the so-called intentional or targeted attacks [30,46,47]), the fraction $1-p$ of the nodes with the highest connectivity is considered as immune and removed together with their outgoing links. The node degree cutoff reduces in this case to the new value $k_{\max}(p)$, which can be estimated from the relation:

$$(1-p) = \sum_{k=k_{\max}(p)}^{k_{\max}} P(k). \tag{8}$$

In turn, the probability $\tilde{p}$ that a link of a given node is leading to a removed node is given by [30] $\tilde{p} = \sum_{k=k_{\max}(p)}^{k_{\max}} kP(k)/\langle k\rangle$, with $\langle k\rangle$ is calculated on the base of the original distribution before the removal of nodes. Thus, as a result of an targeted scenario we have a SF network with the cutoff $k_{\max}(p)$, where the fraction $\tilde{p}$ of nodes are randomly removed. The threshold value of $p_{\rm perc}$ in this situation can be found from the condition (2), where the averages $\langle k\rangle(p)$, $\langle k^2\rangle(p)$ are performed on the base of the distribution function:

$$\tilde{P}(k) = \sum_{m\geq k}^{k_{\max}(p)} P(m)\frac{m!}{k!(m-k)!}(1-\tilde{p})^k\tilde{p}^{m-k} \tag{9}$$

with the upper cutoff $k_{\max}(p)$ estimated from (8).

With the simulated networks at hand, the maximal node degree $k_{\max}(p)$ follows automatically. The estimates for percolation thresholds in this case are evaluated based on Eq. (2) using the averaged values for $\langle k\rangle(p)$ and $\langle k^2\rangle(p)$ found in our simulations: $p_{\rm perc}(\lambda=2.1)=0.76$, $p_{\rm perc}(\lambda=2.5)=0.85$, $p_{\rm perc}(\lambda=2.9)=0.91$ (again, we should mention that these finite-size values are not to be compared with the analytic results obtained for infinite networks as given e.g. in [30]). Note the pronounced increasing of percolation threshold due to removing the nodes with high connectivity, which play the main role in keeping the network structure connected.

The cluster distributions in the case of targeted scenario are shown in Fig. 4, which should be compared with Fig. 3. At $p=0.3$ and $p=0.5$, presented networks are below the percolation threshold, and one observes a large amount of small clusters of susceptible nodes. Only at $p=0.8$, which is close to the percolation threshold of the network with $\lambda=2.1$, we observe an increasing probability for a node to be in a large spanning cluster.

Thus, already at this level of analysis one can immediately conclude about the efficiency of the targeted scenario. Indeed, absence of large connected clusters of susceptible nodes up to $p=0.8$ indicates a severe difficulty for epidemic to spread in such system.

3. The method

With the constructed vaccinated networks at hand, we are in position to analyze the spreading phenomena on such structures. The various spreading scenarios and cellular automaton algorithm which is used to implement these scenarios in a vaccinated network are described below.

3.1. Spreading scenarios

Within compartmental models, that serve a paradigm of epidemic quantitative description [12,13], the system of agents (population) at any stage of spreading process is assumed to contain the three main classes of individuals: susceptible S, infected I, and removed R (either by recovery and acquiring immunity or by death). Each node of the network thus represents an individual, which can exist in three possible states, and each link corresponds to the interaction (contact) between the individuals which allows the disease transmission. Within the mostly simplified SI scenario, once being infected the susceptible individuals stay infected and infectious throughout their life. The SIS model describes the disease without immunity, where individuals can be infected again and again. In this case, the so-called endemic state can emerge: the ratio of infected individuals reaches some equilibrium value, and spreading process continues in time without termination. The SIR model describes the disease with acquired immunity: in response of being infected and cured a person becomes resistant to a given infection during a life time. This mechanism leads to possibility of epidemic outbreak.

In both SIS and SIR cases, the effective spreading rate β (also known in epidemiology as a basic reproduction number [48]) plays an essential role in determining the course of process. An estimate for the threshold value of β for the SIS model on general complex networks is given by [16] :

$$\beta_c^{SIS} = \frac{\langle k\rangle}{\langle k^2\rangle}, \tag{10}$$

where averaging is performed with the corresponding node degree distribution function. Only when effective spreading rate on a given network exceeds β_c, the spreading leads to endemic state, whereas at $\beta<\beta_c$ it stops with time. In the asymptotic limit of infinitely large SF networks, the second moment of the degree distribution (1) diverges at $2<\lambda<3$ and one finds $\beta_c\to 0$, thus confirming the fragility of such networks for disease spreading. Note however that for smaller

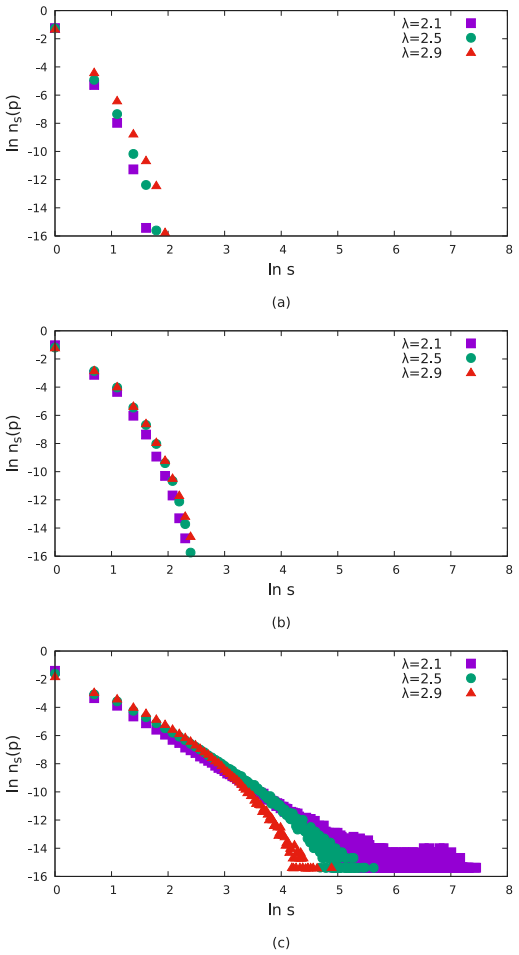

Fig. 4. Number of clusters per network node $n_s(p)$, averaged over an ensemble of network configurations, as a function of cluster size s for a SF network of size $N = 6000$ at various λ and concentrations of susceptible nodes $p = 0.3$ (a), $p = 0.5$ (b), $p = 0.8$ (c) in a double logarithmic scale. The targeted scenario is applied. The large connected component is absent for the low concentrations of susceptible nodes.

size networks $\langle k^2 \rangle$ has a huge but finite value, defining an effective nonzero threshold due to finite size effects, as it is usual in non-equilibrium phase transitions [18]. Correspondingly, for the SIR model the threshold value β_c, which separates the non-spreading state and regime with epidemic outbreak, is given by [17]:

$$\beta_c^{SIR} = \frac{\langle k \rangle}{\langle k^2 \rangle - \langle k \rangle}. \tag{11}$$

Estimate for β_c^{SIR} is directly connected with problem of bond percolation on a corresponding network.

3.2. Updating algorithm

The classical compartment models [12,13] are formulated within the frames of the differential equations and do not take into account the local structure of the system, serving in some sense like a mean-field approximation (each individual is assumed to interact simultaneously with all the other individuals). A more advanced description is provided e.g. by the cellular automaton (CA) means, which is based on the local properties of the system and allows to evaluate the global properties from the local ones. Here, one considers a set of individuals, each being attached to a node of an underlying graph. The evolution of the system is governed by a specific update algorithm, which at each discrete moment of time changes the state of individuals according to the states of their neighbors in the graph.

We consider the synchronous version of CA updating algorithm, where one time step implies a sweep throughout the whole system [49]. At time t, the kth node is considered to be in a state $\sigma_k(t)$, with $\sigma_k(t)$ taking values from a set {0, 1, 2}, corresponding to S, I, or R respectively. Let $S(t)$, $I(t)$ and $R(t)$ be fractions of healthy (susceptible), infected and recovered individuals, located on the nodes of the network, such that $S(t) + I(t) + R(t) = 1$. Thus, the global fractions S, I, and R are

given by:

$$S(t) = \frac{1}{N}\sum_{k=1}^{N}\delta_{0\sigma_k(t)},$$

$$I(t) = \frac{1}{N}\sum_{k=1}^{N}\delta_{1\sigma_k(t)},$$

$$R(t) = \frac{1}{N}\sum_{k=1}^{N}\delta_{2\sigma_k(t)},$$

where δ is the Kronecker delta, N is the total number of agents and summation is performed over all network nodes. To further account for the heterogeneity of a SF network, it has been suggested to consider the probability of a local short-distance disease transmission differing from the spreading rate β [50]:

$$p_k(t) = 1 - (1-\beta)^{n_k(t)}, \tag{12}$$

where $n_k(t)$ is a number of infected nearest neighbors of a node k at time t. The time update $t-1 \to t$ consecutively considers all $k = 1, \ldots, N$ nodes and changes each state $\sigma_k(t-1) \to \sigma_k(t)$ according to the rules described below.

(i) SI model

- Choose node k.
- If $\sigma_k(t-1) = 1$, then do nothing so that $\sigma_k(t) = 1$.
- If $\sigma_k(t-1) = 0$, then the state is changed to 1 with probability $p_k(t-1)$ (Eq. (12)), so that $\sigma_k(t) = 1$.

(ii) SIS model

- Choose node k.
- If $\sigma_k(t-1) = 1$, then it is cured with probability 1 so that $\sigma_k(t) = 0$.
- If $\sigma_k(t-1) = 0$, then the state is changed to 1 with probability $p_k(t-1)$ (Eq. (12)), so that $\sigma_k(t) = 1$.

(iii) SIR model

- Choose node k.
- If $\sigma_k(t-1) = 2$, then do nothing.
- If $\sigma_k(t-1) = 1$, then with probability 1 it is recovered, so that $\sigma_k(t) = 2$.
- If $\sigma_k(t-1) = 0$, then the state is changed to 1 with probability $p_k(t-1)$ (Eq. (12)), so that $\sigma_k(t) = 1$.

As already mentioned above, we will analyze spreading processes in the case, when only a selected fraction p of nodes (agents) is susceptible to disease. To this end, applying the rules of random or targeted scenario, at initial moment of time $t = 0$ we consider each node k of the network to be either susceptible to disease with probability p or immune with probability $1-p$ (the state of corresponding nodes $\sigma_k = 0$ always, and these nodes are considered as non-active in an updating algorithm).

The maximum number of time steps is taken $t = 400$ (typical times for reaching the stationary state for the cases studied below are found in general at $t < 100$).

4. Results

We apply the cellular automaton mechanism to study the epidemic process on networks with fraction p of active nodes, obtained as a result of both random and targeted scenarios, as described in the previous Section. At time $t = 0$, we chose randomly a small fraction $i_0 = 0.01$ of susceptible nodes, which are supposed to be infected. The disease spreading process from infected to susceptible agents is started then.

4.1. SI model

Since the equilibrium values of $I^*(p)$ and $S^*(p)$ do not depend on β in the case of this scenario, we fix the value for the infection rate $\beta = 0.5$ to make the evolution process fast. One can easily estimate the fraction of nodes $S^*(p)$ which remain susceptible and not affected by the spreading process, using the arguments from our previous work on the spreading on regular lattice [28]. Indeed, if at $t = 0$ in some cluster of size s of susceptible agents no one node gets infected, this cluster will remain safe till the epidemic terminates (this cluster will not be touched by the epidemic process in any way). $S^*(p)$ thus equals to the fraction of nodes $P_{\rm safe}(p)$ in these "safe clusters", which can be easily estimated as:

$$S^*(p) = P_{\rm safe}(p) = \sum_s (1-i_0)^s P_s(p). \tag{13}$$

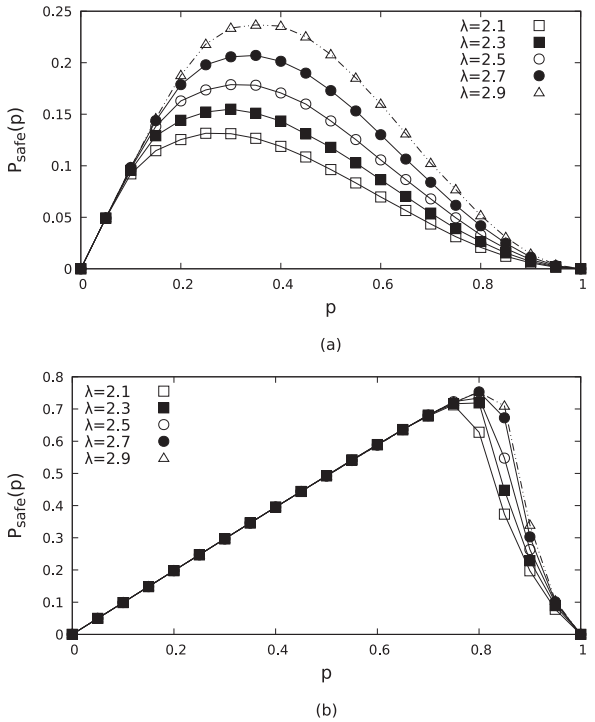

Fig. 5. Numerical values for $P_{\text{safe}}(p)$ (equal to equilibrium values of fraction of susceptible nodes $S^*(p)$ in SI model) as a function of p at different λ in random scenario (a) and targeted scenario (b). The maximum number of individuals not affected by spreading process increases with decreasing the parameter λ.

Here, $P_s(p)$ is the probability to find a cluster containing s susceptible nodes in a network vaccinated according to given scenario (as discussed in Section 2.2), and the sum spans over all available clusters of susceptible nodes. The equilibrium value for the fraction of infected agents is thus straightforwardly given by $I^*(p) = p - S^*(p)$.

The data for $S^*(p)$ obtained in our simulations as results of random and targeted vaccination are presented in Fig. 5. These results can be treated as a direct consequence of performed vaccination, which is not only protecting immunized individuals, but also increases the fraction of susceptible individuals not affected by disease. Note, that for each λ, in both scenarios we obtain a maximum of unaffected individuals at some value of $p_{\max}$, which can be explained based on the same considerations as presented in our previous analysis of regular lattices [28]. To this end, let us recall the cluster size distributions as presented in Figs. 3 and 4. At small values of p (up to some critical one $p_{\max}$), there is a large amount of clusters of small size, and "diversity" of clusters (number of different clusters) increases with p. Thus, the probability for one of them to get infected gets lower and that is why $P_{\text{safe}}(p)$ increases in this region. On the other hand, above the value of $p_{\max}$ the number of various clusters decreases (small clusters start to segregate into the larger ones), which in turn makes it easier for infection to propagate through the system (thus also $P_{\text{safe}}(p)$ starts to decrease). For the networks under consideration, in the case of random scenario $p_{\max}$ is found to be around 0.3, whereas for the case of targeted scenario it is observed to be around 0.8.

Note, that in the case of random scenario, the number of unaffected nodes strongly depends also on the parameter λ. Again, recalling the cluster distribution as shown on Fig. 3, the smaller the parameter λ, the larger the probability for a big cluster of susceptible nodes to occur, which makes the system more fragile for infection spreading. Indeed, $S^*(p)$ decreases with decreasing λ. The situation is very different in the case of the targeted scenario, where there is practically no difference in $P_{\text{safe}}(p)$ in the case of strong vaccination (for p below 80%). It can be explained by the fact, that the main qualitative difference between networks with different λ is caused by presence of hubs, which are stronger and make the system more connected, the smaller is parameter λ. Removing the hubs from spreading process by vaccinating them leads to breaking the connectivity of network, which now consists of a large number of disconnected clusters of small sizes, as shown in Fig. 3. In this respect, there is practically no difference in cluster distribution at various λ. Comparing the data of Fig. 5, one immediately notices the effectiveness of targeted vaccination. Indeed, in this case the maximum number of individuals, not affected by disease, reaches almost 80% of population at corresponding $p_{\max}$ value and is almost independent on λ, whereas in the case of random vaccination it does not exceed 25%.

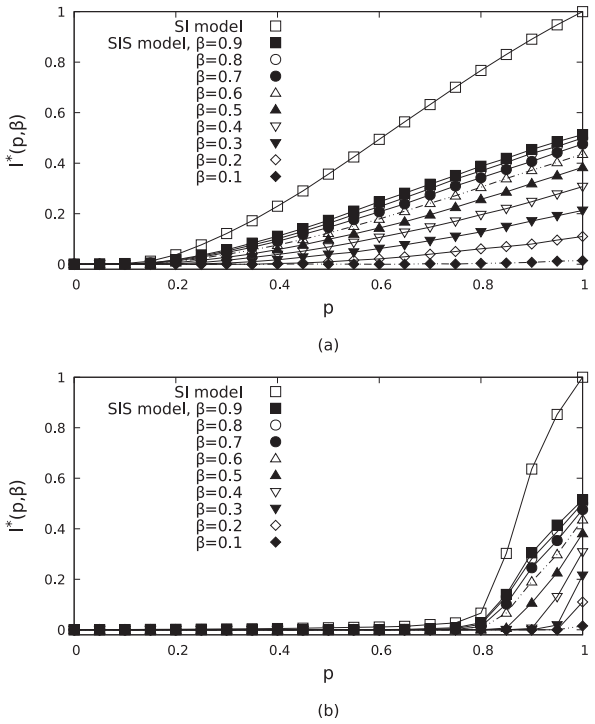

Fig. 6. Total fraction of infected nodes in equilibrium as function of p for a SF network with $\lambda = 2.5$ for the SI (open squares) and SIS (all other symbols at different β) models. Lines are guides to the eye. (a) Random scenario, (b) targeted scenario.

4.2. SIS model

Within the frames of SIS scenario, the infected individuals get cured without obtaining immunity, so that they can be infected over and over again, undergoing a cycle $S \to I \to S$. After reaching the equilibrium state, one obtains the values $S^*(p, \beta)$ and $I^*(p, \beta)$ for the fractions of susceptible and infected individuals, which now are defined not only by the initial amount of susceptible individuals p, but also by the spreading rate β.

We start with analyzing the averaged amount of infected nodes, which can be observed in a network in equilibrium state. In Fig. 6 we give the example of our numerical estimates for the case $\lambda = 2.5$, applying both the random and targeted scenarios of vaccination. As expected, $I^*(p, \beta)$ in both cases is considerably smaller compared to the simplified SI model and decreases with lowering the spreading rate β. These data allow us to directly compare the effectiveness of two types of vaccinations. Let us recall that the minimum fraction $p_c(\beta)$ of susceptible individuals, at which the infection can "survive' in a system (the value of $I^*(p, \beta)$ is above zero), can be estimated as [29]:

$$\frac{\langle k\rangle(p = p_c)}{\langle k^2\rangle(p = p_c)} = \beta, \tag{14}$$

where the averages $\langle k\rangle(p)$, $\langle k^2\rangle(p)$ are performed with the degree distribution of the network resulting after the removal of the $(1 - p)N$ nodes of highest degree.

Making use of the data for $\langle k\rangle$, $\langle k^2\rangle$ obtained in our simulations, we have for example at $\lambda = 2.5$: $p_c(\beta = 0.6) = 0.15$, $p_c(\beta = 0.3) = 0.3$, $p_c(\beta = 0.1) = 0.91$. For the case of targeted vaccination, making use of Eq. (14) gives us corresponding estimates: $p_c(\beta = 0.6) = 0.75$, $p_c(\beta = 0.3) = 0.85$, $p_c(\beta = 0.1) = 1.0$, so that one observes a non-zero value of $I^*(p, \beta)$ at considerably larger values of p comparing to the random scenario. One observes no spreading activity ($I^*(\beta, p)$ is practically zero) in this case at $p < 0.8$ even at very strong disease spreading rate (large β). Such a quantitative difference between two scenarios can be intuitively understood, recalling the peculiarities of distribution of clusters of susceptible nodes (as described in Section 2.2). Indeed, at the same value of p, targeted scenario leads to formation of a large amount of separated clusters of very small size, as compared with the random scenario. This leads to restriction of infection in very small separated regions and preventing its spreading around in spanning clusters, as it takes place during the random vaccination scenario.

Analysis of system behavior at various values of parameter β reveals a kind of phase transition between the so-called endemic state (with non-zero equilibrium value of $I^*(p, \beta)$) and disease-free states, where the role of the order parameter is played by the stationary value of $I^*(p, \beta)$. The phase diagrams of corresponding phase transitions are given

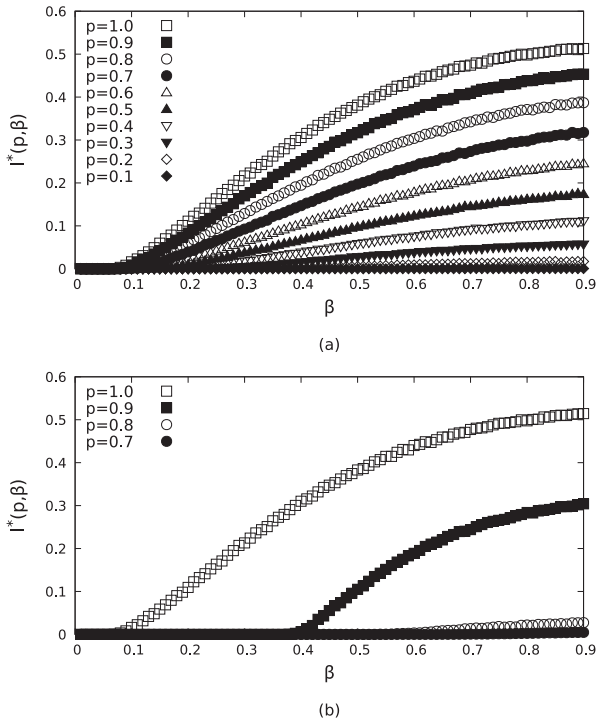

Fig. 7. Total fraction of infected nodes in equilibrium for a SF network with $\lambda = 2.5$ for the SIS model as function of β. (a) Random scenario, (b) targeted scenario.

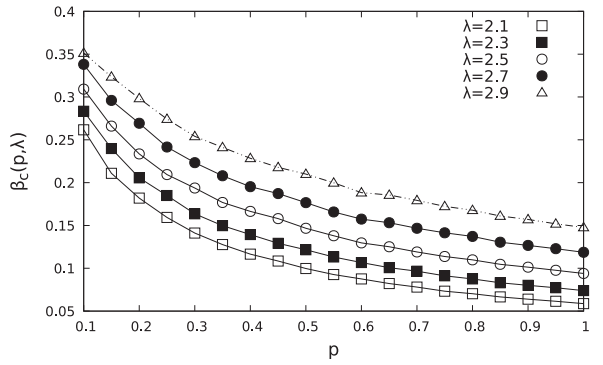

Fig. 8. Critical value of spreading rate $\beta_c(p, \lambda)$ for a SF network in SIS model in a random scenario.

in Fig. 7. The critical value of the effective spreading rate $\beta_c(p, \lambda)$ is defined as those separating infected and healthy phases. We obtained the numerical estimates for $\beta_c(p, \lambda)$ by making use of fitting of data for $I^*(p, \beta)$ to the form $I^*(p, \beta) = A(\beta_c(p, \beta) - \beta)^\gamma$, where A is constant. The results are presented in Fig. 8. Note that at $p = 1$ the results for β_c are in a good correspondence with estimates based on Eq. (10) and with the numerical simulations performed in [25]. Note that we present the results for β_c only for the case of random vaccination scenario, since for the targeted scenario for p above 0.8 practically no infection activity is observed in system even at very high values of spreading rate β.

As expected, the threshold value of $\beta_c(p, \lambda)$ increases with decreasing parameter p: infection should be "stronger" to occupy the system, if fraction of vaccinated individuals increases. On the other hand, $\beta_c(p, \lambda)$ decreases with decreasing the parameter λ. It is connected with the fact, that the smaller the λ, the larger is the probability to find high-degree nodes in the network. This makes the spreading of infection on such networks much more easier.

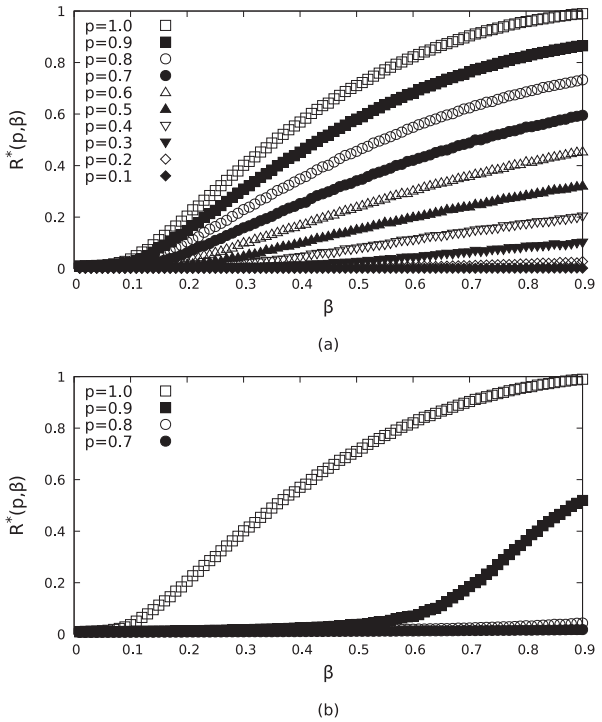

Fig. 9. Total fraction of removed nodes in equilibrium for a SF network with $\lambda = 2.5$ for the SIR model as a function of β. (a) Random scenario, (b) targeted scenario.

4.3. SIR model

Within the frames of SIR scenario, which can be described by a simple scheme $S \to I \to R$, the infected individuals get immune, so that the repeated infection of the same node is not allowed in the course of such process. After reaching the equilibrium state, the fraction $R^*(p, \beta)$ of individuals becoming removed (or with the life-long immunity) is observed (obviously $I^*(p, \beta)$ is always zero in this scenario, independently on details of the epidemic spreading). The rest of individuals ($S^*(p, \beta) = p - R^*(p, \beta)$) remain susceptible.

The SIR model also exhibits a transition between a phase where the disease outbreak reaches a finite fraction of the population and a phase where only a limited number of individuals is affected. The order parameter is therefore the density of removed individuals in an equilibrium state, which is defined by the effective spreading rate β_c, separating infected and healthy phase. The phase diagrams of corresponding phase transitions are given in Fig. 9. Qualitatively, the picture resembles the transition between endemic and healthy states within the frames of SIS model (Fig. 7). Again, for the case of targeted vaccination one observes a non-zero value of $R^*(p, \beta)$ at considerably larger values of p comparing with the random scenario, and there is no spreading activity ($R^*(\beta, p)$ is practically zero) in this case at $p < 0.8$ even at very strong disease spreading rate (large β).

Our numerical estimates for $\beta_c(p, \lambda)$ for the case of random scenario are presented in Fig. 10. At $p = 1$ the results for β_c are in a good correspondence with the estimates based on Eq. (11). Similarly to the case of SIS scenario, the threshold values of $\beta_c(p, \lambda)$ increase with decreasing parameter p and decrease with decreasing λ. Note also, that at each p and λ values the epidemic spreading for the SIS model occurs at a smaller value of β_c comparing with the SIR model. In the latter case, the susceptible individuals cannot be infected multiple times, which effectively makes the spreading process more weak as comparing with the SIS scenario.

5. Conclusions

The goal of our study was to reveal peculiarities of infection spreading in the environment comprising agents of two types: those that can be a subject of infection and those that do not participate in the spreading, being "immune". To this end, we considered a model in which only some fraction p of agents-nodes are susceptible to the disease transmission, whereas the other $1 - p$ are treated as immune (vaccinated). In this respect, the present work continues our previous study [28], where the similar situation was analyzed on the background of a regular square lattice. One of the crucial points there was the emergence of the so-called safety patterns of susceptible sites, surrounded by immune ones, which

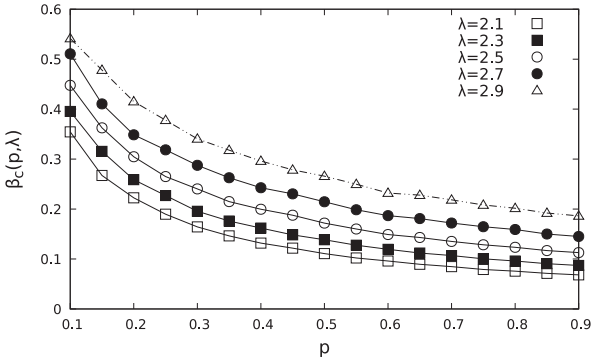

Fig. 10. Critical value of spreading rate $\beta_c(p, \lambda)$ for a SF network in SIR model in a random scenario.

remain unaffected by disease until the stationary state is reached. Detailed analysis of safety pattern distribution thus enables one to determine the fraction of infected agents in a stationary state. In the present study we aim to extend this analysis to the case of a more complex underlying structures. To this end, it is natural to choose the SF networks, which are more closely related to real world situations. The question of interest is the impact of local heterogeneity of such structures on the safety pattern distribution and thus on the peculiarities of spreading processes in such systems.

With the said above in mind, we have modeled the spreading process on SF networks with node degree distribution given by Eq. (1) with the decay exponent λ ranging within $2 < \lambda < 3$. The dynamics of spreading phenomena on such structures is of interest in many aspects, examples ranging from computer virus infections to epidemic diseases. Due to the heterogeneity of SF networks, two immunization scenarios have been applied. In the simplest random immunization (as exploited in our previous study of a regular lattice), a share of nodes is randomly chosen and made immune. More effective targeted scenario implies the targeting the highest degree nodes. To generate vaccinated networks, we made use of the so-called configuration model.

It is worth noting that the effects under consideration cannot be studied within traditional analysis of compartmental models based on the homogeneous mixing hypothesis and the differential equation approach [12]. There, the local structure is excluded from consideration and only the global macroscopic features can be catched. On the other hand, the microscopic analytic treatment is highly complicated due to the strong heterogeneity of the agent-based model under consideration. In such situation, it is optimal to use the cellular automaton approach, based on thorough taking into account details of local interactions between agents on the microscopic scale. Within this approach, we have implemented three basic spreading scenarios (SI, SIS and SIR) for variable ratio ($0 \leq p \leq 1$) of susceptible nodes. We studied the susceptible clusters (the safety patterns) distributions in the case of both random and targeted scenarios. It has been analyzed, how the removing of even the small fraction of the highest degree nodes within the latter scheme results in corrupting the spanning clusters and thus preventing the infection spreading. The main impact of the heterogeneous structure of the underlying network manifests itself already on this level of analysis. Whereas for the random scenario the fraction of nodes in safety patterns in a SF network is qualitatively comparable with those of the regular network, the targeted scenario leads to the pronounced increase of the number of such nodes (cf. Fig. 5 of the present study and Fig. 3 of Ref. [28]). Already within the frames of simplified SI model, one notices the effectiveness of a targeted vaccination: e.g. at $\lambda = 2.5$ the maximal amount of individuals, not affected by disease, reaches almost 80% of population. Note that in the case of random vaccination it does not exceed 25%. Similar picture was observed while analyzing SIS and SIR models: within the targeted scenario, the spreading process was shown to be prevented at $p < 0.8$ even at very strong disease spreading rate (large β).

The numerical estimates for the threshold values of spreading parameters $\beta_c(p, \lambda)$ have been obtained within SIS and SIR models within the frames of random scenario. In both cases, $\beta_c(p, \lambda)$ increase with decreasing parameter p. This is intuitively understood since when the fraction of vaccinated individuals increases, the infection has to be "stronger" to occupy the whole system. On the other hand, the heterogeneity of the SF network, which is more pronounced with an increase of λ, leads to decrease of the threshold value of $\beta_c(p, \lambda)$ (as shown in Fig. 8). Again, one can compare these results with the corresponding values obtained in our previous study (Fig. 11 of Ref. [28]). This leads to the conclusion that within a random scenario, a SF network is more compliant for disease spreading as comparing with the regular lattice structure, and this effect is more pronounced with increasing the parameter λ. On the other hand, vaccination within the targeted scenario makes SF networks incomparably more resistant to epidemic spreading than the regular lattice structures.

CRediT authorship contribution statement

V. Blavatska: Methology, Conceptualization, Software, Writing – original draft. **Yu. Holovatch:** Supervision, Formal analysis, Writing – review & editing.

Declaration of competing interest

The authors declare that they have no known competing financial interests or personal relationships that could have appeared to influence the work reported in this paper.

Acknowledgments

This work was supported in part by National Research Foundation of Ukraine, project "Science for Safety of Human and Society" No. 2020.01/0338 (VB) and by the National Academy of Sciences of Ukraine, project KPKBK 6541030 (YuH).

References

[1] C. Moore, M.E.J. Newman, Phys. Rev. E 61 (2000) 5678.
[2] W.H. Murray, Comput. Secur. 7 (1988) 139.
[3] M.E.J. Newman, S. Forrest, J. Balthrop, Phys. Rev. E 66 (2002) 035101(R).
[4] D.J. Daley, D.G. Kendal, J. Inst. Math. Appl. 1 (1965) 42.
[5] J.D. Murray, Mathematical Biology, Springer Verlag, Berlin, 1993.
[6] A.-L. Barabási, R. Albert, Science 286 (1999) 509.
[7] M. Faloutsos, P. Faloutsos, C. Faloutsos, Comput. Commun. Rev. 29 (1999) 251.
[8] G. Caldarelli, R. Marchetti, L. Pietronero, Euro-Phys. Lett. 52 (2000) 386.
[9] K.-I. Goh, B. Kahng, D. Kim, Phys. Rev. Lett. 88 (2002) 108701.
[10] M.E. Newman, Phys. Rev. E 64 (2001) 016131.
[11] A.F. Naviaa, V.H. Cruz-Escalonac, A. Giraldob, A. Barausse, Ecol. Model. 328 (2016) 23.
[12] W.O. Kermack, A.G. McKendrick, Proc. R. Soc. Lond. Ser. A Math. Phys. Eng. Sci. 115 (1927) 700.
[13] R.M. Anderson, R.M. May, Infectious Diseases in Humans, Oxford University Press, Oxford, 1992.
[14] R. Pastor-Satorras, A. Vespignani, Phys. Rev. Lett. 86 (2001) 3200.
[15] R. Pastor-Satorras, A. Vespignani, Phys. Rev. E 63 (2001) 066117.
[16] R. Pastor-Satorras, A. Vespignani, Phys. Rev. E 65 (2002) 035108R.
[17] R. Pastor-Satorras, C. Castellano, P. Van Miegh, A. Vespignani, Rev. Modern Phys. 87 (2015) 925.
[18] J. Marro, R. Dickman, Nonequilibrium Phase Transitions in Lattice Models, Cambridge University Press, Cambridge, 1999.
[19] M. Boguñà, R. Pastor-Satorras, Phys. Rev. E 66 (2002) 047104.
[20] Y. Moreno, R. Pastor-Satorras, A. Vespignani, Eur. Phys. J. B 26 (2002) 521.
[21] Y. Moreno, A. Vázquez, Eur. Phys. J. B 31 (2003) 265.
[22] M. Barthèlemy, A. Barrat, R. Pastor-Satorras, A. Vespignani, J. Theoret. Biol. 235 (2005) 275.
[23] P. Van Mieghem, R. van de Bovenkamp, Phys. Rev. Lett. 110 (2013) 108701.
[24] S. Chatterjee, R. Durrett, Ann. Probab. 37 (2009) 2332.
[25] S.C. Ferreira, C. Castellano, R. Pastor-Satorras, Phys. Rev. E 86 (2012) 041125.
[26] A.S. Mata, S.C. Ferreira, Europhys. Lett. 103 (2013) 48003.
[27] P. Fine, K. Eames, D.L. Heymann, Clin. Infect. Dis. 52 (2011) 911.
[28] V. Blavatska, Yu Holovatch, Physica A 573 (2021) 125980.
[29] R. Pastor-Satorras, A. Vespignani, Phys. Rev. E 65 (2002) 036104.
[30] R. Cohen, K. Erez, D. ben Avraham, S. Havlin, Phys. Rev. Lett. 86 (2001) 3682.
[31] R. Cohen, S. Havlin, D. ben Avraham, Phys. Rev. Lett. 91 (2003) 247901.
[32] P. Holme, B.J. Kim, C.N. Yoon, S.K. Han, Phys. Rev. E 65 (2002) 056109.
[33] P. Holme, Europhys. Lett. 68 (2004) 908.
[34] E.A. Bender, E.R. Canfield, J. Combin. Theory Ser. A 24 (1978) 296.
[35] M. Molloy, B. Reed, Random Struct. Algorithms 6 (1995) 161.
[36] M. Molloy, B. Reed, Combin. Probab. Comput. 7 (1998) 295.
[37] R. Cohen, K. Erez, D. ben Avraham, S. Havlin, Phys. Rev. Lett. 85 (2000) 4626.
[38] M. Catanzaro, M. Boguñá, R. Pastor-Satorras, Phys. Rev. E 71 (2005) 027103.
[39] J. Hoshen, R. Kopelman, Phys. Rev. E 14 (1976) 3438.
[40] V. Blavatska, W. Janke, J. Phys. A 42 (2009) 015001.
[41] S. Yu Lapshina, Lobachevskii J. Math 40 (2019) 341.
[42] M. Kotwica, P. Gronek, K. Malarz, Internat. J. Modern Phys. C 30 (2019) 1950055.
[43] F.C. de Oliveira, S. Khani, J.M. Maia, F.W. Tavares, Mol. Simul. 46 (2020) 1453.
[44] D. Stauffer, A. Aharony, Introduction To Percolation Theory, Taylor and Francis London, 1992.
[45] M.F. Sykes, M. Glen, J. Phys. A: Math. Gen. 9 (1976) 87.
[46] B. Berche, C. von Ferber, T. Holovatch, Yu Holovatch, Eur. Phys. J. B 71 (2009) 125.
[47] B. Berche, C. von Ferber, T. Holovatch, Yu Holovatch, Adv. Complex Syst. 15 (2012) 1250063.
[48] G.N. Milligan, D.T. Barrett, Vaccinology: An Essential Guide, Chichester, Wiley Blackwel, West Sussex, 2015.
[49] P. Grassberger, Math. Biosci. 63 (1983) 157.
[50] H.F. Gagliardi, D. Alves, Math. Popul. Stud. 17 (2010) 79.